Scientia Iranica, Vol. 15, No. 4, pp 457–468
© Sharif University of Technology, August 2008

SCIENTIA
IRANICA

Application of Response Surface Methodology in Study of the Product Yield Distribution of Thermal Cracking of Atmospheric Gasoil

S.Z. Abghari[1], J. Towfighi[1,*], R. Karimzadeh[1] and M. Omidkhah[1]

In order to determine the yield distribution of thermal cracking of gasoil, a pilot plant was designed and setup. A systematic experimental design was utilized based on CCD (central composite design). The feed flow rate, steam ratio and temperature were considered as factors to design the experiments. Some statistical models were tuned based on the results of conducted experiments. The models were evaluated with lack-of-fit and R-squared tests. The results of the analysis proved that the models fitted well with the experimental results of the considered products. Based on the experiments and statistical models the pilot plant was optimized in order to maximize the net profit. At the optimum point coil outlet temperature, the feed flow rate and steam ratio were, respectively, equal to 843.8°C, 6.02 g/min and 0.46. Regarding these conditions, the yield of ethylene, propylene and butadiene and rate of coke formation would be 23.82 wt%, 12.13 wt%, 2.42 wt% and 14.44×10^{-7} g/cm^2.sec, respectively.

INTRODUCTION

Pyrolysis, or steam cracking, is the main process for production of ethylene, propylene and other light olefins. In this process, hydrocarbon feed is introduced into a tubular reactor, in which temperature is high and residence time is short. However, steam should be used to increase the olefin selectivity. In addition, this is used to reduce the coke formation by decreasing hydrocarbon partial pressure [1,2]. In this process, the value of steam ratio depends on the feedstock. While the range for ethane and propane can be determined as being between 0.3 to 0.4, the range for naphtha would be 0.6 to 0.7. The diluted feed is preheated close to cracking temperature, depending on the hydrocarbon feed type.

Coke formation is always accompanied by the pyrolysis of hydrocarbon. The coke deposits on the inner surface of the reactor tube wall and the deposition not only affects heat transfer, but also increases the pressure drop of the fluid. It also increases hot spot formation and would decrease the operating cycle and the capacity of the plant as well [3].

The Paraffinic feedstock is thermally cracked into mainly olefins, aromatics, methane and hydrogen. The homogeneous cracking reactions are endothermic. As such, energy is required to elevate the gas temperature to about 700-875°C at the outlet of the reactor coils [4,5].

Common feedstocks for this unit are paraffinic hydrocarbons in the ranges between ethane to naphtha. Rising naphtha prices and the demand for lighter hydrocarbons have caused the propensity of the higher boiling petroleum fractions to act as feedstock for olefin production. For this purpose, gasoils are the main choice.

Different authors have studied the product yield distribution of the thermal cracking of gasoils and the effects of different parameters on this [6-10]. Zdonik et al. [6] introduced some parameters, which are important in the characterization of gasoil in the thermal cracking process. These parameters are BMCI, molecular weight and hydrogen content.

Kaiser et al. [7] reported the yield distribution of the thermal cracking of several feedstocks, including ethane, propane, butanes, full range naphtha cuts and atmospheric gasoil. They have also proved that the feedstock affects ethylene production costs by impress-

---

1. *Department of Chemical Engineering, Faculty of Engineering, Tarbiat Modares University, P.O. Box: 14115-143, Tehran, Iran.*

*. *To whom correspondence should be addressed. E-mail: Towfighi@modares.ac.ir*

ing the product slate, utility consumption and plant investment. According to their report, the yield of ethylene production goes from 80 percent for ethane to 25 percent for gasoil.

Depeyre et al. [8] studied the product yield distribution of the thermal cracking of atmospheric gasoil. Several experiments were conducted in tubular quartz and inconel reactors. The study was carried out in order to determine the effects of temperature, steam ratio and residence time.

Clymans et al. [9] collected extensive data on the thermal cracking of various fractions resulted from the hydrotreatment of virgin vacuum gasoil. The fractions consist of Hydrotreated naphtha (I.B.P-175°C), hydrotreated kerosene (175-250°C), hydrotreated atmospheric gasoil (250-350°C) and hydrotreated vacuum gasoil (350°C+). The potential of these fractions was evaluated as feedstock for olefin production. They determined that the heavy hydrotreated fraction (HVGO) was a valuable alternative for straight run naphtha.

In industrial scale processes, several modifications were conducted to improve the productivity of the thermal cracking of gasoils. Wernicke et al. [10] invented thermal cracking with a pretreatment section. They introduced a process containing primary hydrogenation of heavy gasoil, followed by thermal cracking. The light products of the hydrogenation section are enriched in branched isomers used as fuel, and the heavy fractions are sent to the steam cracking section. In the developed process, hydrogenation will be performed in conditions under which the polyaromatics are extensively hydrogenated.

This paper focuses on the yield distribution of the thermal cracking products of atmospheric gasoil. The effects of temperature, steam ratio and feed flow rate are determined by a series of experiments, designed via the use of CCD (Central Composite Design). By applying the response surface methodology, ANOVA and related statistical tests, statistical models are developed and evaluated. Concerning the developed model, an optimization is carried out to determine the operating conditions and, accordingly, to maximize the net profit.

EXPERIMENTAL SECTIONS

Feed Characteristics

The selected atmospheric gasoil had a boiling range of 218°C to 387°C, with a density of 0.845 gr/cm^3. The main properties of this hydrocarbon feed are listed in Table 1.

The BMCI and coking inhibition index of the selected atmospheric gasoil are, respectively, 28.26 and 36.75, showing a low coking intensity [11].

Table 1. The main properties of atmospheric gasoil.

Specification	Gas-Oil
Sulfur, total wt%	0.75
Nitrogen, total wt%	< 0.5
Hydrogen, total wt%	13.8
Carbon, total wt%	85.6
Aromatic content vol%	14
Olefin content vol%	Trace < 0.3
Saturate content vol%	86
Distillation:	°C
IBP at 760mm Hg	218
5% vol. recovery	257
10% vol. recovery	266
30% vol. recovery	285
50% vol. recovery	303
70% vol. recovery	324
90% vol. recovery	362
FBP at 760 mm Hg	387

Pilot Plant Setup

The experiments have been carried out in a pilot set up, designed and assembled for the hydrocarbon feed stocks in the range from ethane to gasoil. This pilot can be fed by liquid or gas hydrocarbons. Liquid hydrocarbons and dilution water have been fed by means of dosing pumps. The feed flow rates and steam ratio can be varied from 1 to 15 gr/min and from 0.3 to 1.0. The schematic diagram of the pilot plant is demonstrated in Figure 1.

The hydrocarbon and dilution water are heated close to cracking temperature (550°C).The reactor furnace has been divided into three zones, which can be heated independently to control the temperature profile. The reactor is 1 m in length, 12 mm in internal diameter and is made of inconel 600. There are twelve thermocouples along the reactor; six inside the furnace, four on the tube skin and two additional thermocouples for measuring the XOT (crossover temperature) and COT (Coil Outlet Temperature).

The reactor effluent would be immediately quenched by cooling water in a double pipe heat exchanger. In order to separate the condensate from the gaseous product stream, the exchanger outlet stream is sent to a flash drum. Then, the gas phase enters a series of condensers, passing through a filter in the final stage. An on-line computer controls the unit. The connection is made through the analog to digital (A/D), digital to analog (D/A) converters and digital input-outputs. In the control part of the preheater and the main furnace, the fluid temperature profile in the preheater and reactor pipes is stabilized by

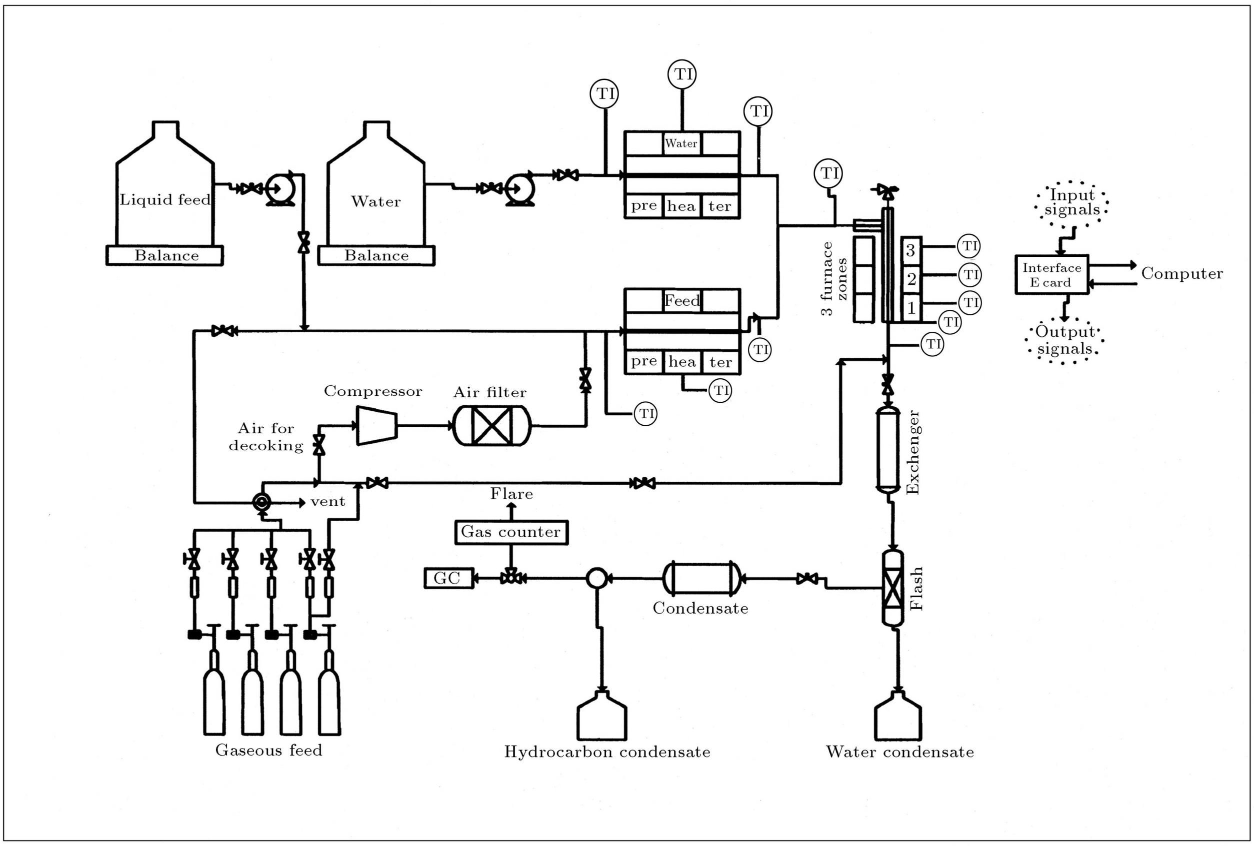

Figure 1. Schematic diagram of the pilot plant setup.

temperature controlling in each zone. PID controllers, which were tuned using an open loop response, are used for system controlling. The controller parameters are 0.1 for proportional gain, 0.004 min for integral time and factors are shown in Table 2. 0.0001 for derivative time for the thermal cracking of the selected atmospheric gasoil. All pilot plant measurements and control system data are saved in the text and graphical mode.

After each run, a fraction of product gas is then withdrawn for analysis via a Varian Chrompack CP3800 gas chromatograph.

STATISTICAL DESIGN OF EXPERIMENTS

A central composite design [12] was applied with three design factors, namely, the hydrocarbon feed flow rate (X_1), the steam ratio (X_2) and coil outlet temperature (X_3).The coded levels and the natural values of the mentioned

Eleven response variables are considered. They include the product yield of primary products and the rate of coke formation. The number of trials was based on the number of design factors and was equal to 19 experiments (15 combinations with four replications). The following full quadratic model was obtained by a multiple regression technique for three factors (Table 2). In order to calculate the coefficients of the model, a MINITAB software (Release 13.2) has been used:

$$Y_i = \alpha + \beta_1 X_1 + \beta_2 X_2 + \beta_3 X_3 + \beta_{11} X_1^2 + \beta_{22} X_2^2 + \beta_{33} X_3^2 + \beta_{12} X_1 X_2 + \beta_{13} X_1 X_3 + \beta_{23} X_2 X_3. \quad (1)$$

The results of the experiments and the design matrix

Table 2. Coded and natural levels of the design factors.

Design Factors	-1.6818	-1	0	1	1.6818
X_1: Feed Flow Rate	0.977	2	3.5	5	6.02
X_2: Steam Ratio	0.46364	0.6	0.8	1.0	1.13636
X_3: Coil Outlet Temperature	716	750	800	850	884

Table 3. Design matrix and results of the central composite design.

No	1	2	3	4	5	6	7	8	9	10	11	12	13	14	15	16	17	18	19
X_1	-1	-1	-1	-1	1	1	1	1	-1.68	1.68	0	0	0	0	0	0	0	-1	-1
X_2	-1	-1	1	1	-1	-1	1	1	0	0	-1.68	1.68	0	0	0	0	0	1	1
X_3	-1	1	-1	1	-1	1	-1	1	0	0	0	0	-1.68	1.68	0	0	0	1	1
Y_1 (C_2H_4)	11.6	26.5	10.2	26.9	6.9	26.7	2.1	20.8	17.8	9.58	21.4	15.1	1.7	30.8	18	17.7	17.2	26.6	26.5
Y_2 (C_3H_6)	7.9	11.6	6.63	12.2	3.39	12.2	1.37	10.2	10.02	7.3	9.8	9.56	0.26	10.7	9.59	8.79	9.74	11.3	10.66
Y_3 (CH_4)	3.7	9.8	3.1	8.99	2.39	8.83	0.58	5.55	7.5	4.6	9	3.79	2.24	10.7	5.24	5	4.74	9.02	8.96
Y_4 (C_3H_8)	0.36	0.4	6.63	0.4	0.18	0.44	0.08	0.37	0.4	0.33	0.48	0.43	0.35	0.35	0.39	0.35	0.38	0.38	0.34
Y_5 (C_2H_6)	1.7	2.3	1.34	2.04	1.04	2.5	0.27	1.52	2.11	1.56	2.54	1.33	1.31	2	1.67	1.71	1.66	2.07	2
Y_6 (C_2H_2)	1.02	0.86	1.21	1.21	0.43	1.27	0.21	0.63	0.74	1.04	0.88	1.98	0.41	1.15	1.46	1.36	1.32	0.96	0.98
Y_7 (C_4H_6)	1.62	5.65	1.68	4.8	1.05	3.6	0.52	3.05	2.51	0.33	3.61	2.41	1.37	7.1	2.11	2.24	2.1	4.93	5.03
Y_8 (C_4H_8)	1.85	2.5	2.07	2.8	1.6	2.31	0.24	0.17	1.81	0.6	3.82	2.73	1.35	2.67	2.05	1.77	1.61	2.42	3.16
Y_9 (H_2)	0.6	1.4	1.6	0.72	0.27	0.92	0.11	0.6	3.9	0.5	4.6	1.58	0.23	1.3	0.54	0.45	0.48	1.04	0.81
Y_{10} (C_{5+})	69.4	36.4	71.2	38.3	84.3	41.1	94.8	53.3	54.60	65.7	43.44	58.6	88.32	32.2	57.7	60.4	60.3	32.1	33.40
Rate of Coke ($gr/cm^2.sec$) $\times 10^7$	1.67	34.1	0.66	20.9	0.16	18.2	0.03	3.9	12.3	0.51	11.53	0.65	0.06	32.4	1.6	2.35	2.40	24.6	25.6

are shown in Table 3. Production yields of hydrogen, acetylene, light olefins and light paraffins, as ethylene, propylene, butadiene, butenes, methane, ethane, propane and rate of coke formation, are taken as response variables.

In Table 4, the significance of different factors and their interactions, the related coefficients, the ANOVA results for lack-of-fit and the result of R-squared tests have been shown. The effects of the parameters with a p-value higher than 0.05 were insignificant. Therefore, they could be discarded with a confidence level of 95%. The lack-of-fit test was used to determine whether or not the constructed model was appropriate to describe the observed data. When the p-value for the lack-of-fit is less than 0.05, there is a statistically significant lack-of-fit at the 95% confidence level, which means that the model does not adequately represent the data. The R-squared statistic indicates the variability percentage of the optimization parameter explained by the model [13].

Derived coefficients were adapted to Equation 1 and demonstrated the general form of a quadratic equation.

As Table 4 provides, some terms were dropped in the acetylene and C5+ developed yield models. This was due to applying step wise [13] regression in the model development. This regression method was utilized to improve the lack of fit and R-squared results. In this regression method, the least significant terms were removed until the R-squared and lack of fit tests showed acceptable results and the majority of the remaining terms were significant.

RESULTS AND DISCUSSION

According to the developed statistical models, the surfaces and contours of the yield of ethylene, propylene, butadiene, butenes and the rate of coke formation, as important response variables, are shown in Figures 2 to 14.

As shown in Figure 2, the maximum yield of ethylene reaches 32% at a feed flow rate of 4 to 4.5 g/min and a steam ratio of 0.4 to 0.46, where COT is at 884°C. Precise analysis of the data confirms that the maximum point is 32.03%, where the feed flow rate is 4.232 g/min and the steam ratio is 0.46.

Table 4. Test of significance of factors and interactions for models of selected parameters, R-squared and lack-of-fit.

Factor or Interaction	**Y_1 (Ethylene Yield)**			**Y_2 (Propylene Yield)**			**Y_7 (Butadiene Yield)**			**Y_8 (Butenes Yield)**			**Rate of Coke Formation $\times 10^7$(gr/cm^2.sec)**		
	Coef.	***T***	**P-Value**	**Coef.**	***T***	**P-Value**	**Coef.**	***T***	**P-Value**	**Coef.**	***T***	**P-Value**	**Coef.**	***T***	**P-Value**
Constant	-196.2	-3.15	0.014	-303.1	-3	0.017	139.07	5.348	0.001	-13.712	-0.11	0.914	968.57	7.231	0
X_1	-5.61	-2.21	0.058	-11.84	-2.7	0.026	4.133	3.485	0.008	4.5277	3.122	0.014	38.013	5.41	0
X_2	-10.55	-0.57	0.586	-16.9	-0.5	0.603	-7.1124	-0.84	0.425	-5.033	-0.64	0.541	193.05	3.796	0.004
X_3	0.41	2.684	0.028	0.8	3.18	0.013	-0.3805	-5.87	0	0.021608	-0.01	0.492	-2.92	-8.838	0
$X_1 \times X_1$	-0.56	-6.33	0	-0.0853	-0.6	0.565	-0.1342	-3.29	0.011	-0.13759	-1.90	0.093	0.47689	2.093	0.066
$X_2 \times X_2$	0.465	0.188	0.856	0.4866	0.1	0.923	3.1354	2.883	0.02	5.8868	4.047	0.004	16.388	2.438	0.037
$X_3 \times X_3$	-2E-04	-2	0.081	-0.0005	-3.2	0.012	0.00027	6.454	0	-4.3E-06	0.16	0.877	0.002193	10.442	0
$X_1 \times X_2$	-4.24	-4.96	0.001	-2.2165	-1.6	0.154	-0.2152	-0.6	0.563	-2.1465	-4.48	0.002	-0.6494	-0.294	0.775
$X_1 \times X_3$	0.0139	4.566	0.002	0.01667	3.25	0.012	-0.0043	-3.09	0.015	-0.00299	-1.93	0.09	-0.05453	-6.517	0
$X_2 \times X_3$	0.0221	0.995	0.349	0.02783	0.76	0.469	0.0022	0.204	0.843	0.002327	0.389	0.707	-0.28708	-4.795	0.001
R-Squared	99.80%			95.50%			99%			93.90%			99.10%		
P-Value of Lack-of-Fit	0.15			0.277			0.072			0.66			0.073		
Factor or Interaction	**Y_2 (CH_4)**			**Y_9 (H_2)**			**Y_6 (C_2H_2)**			**Y_{10} (C5+)**			**Yield of Light Paraffins (Ethane & Propane)**		
	Coef.	***T***	**P-Value**	**Coef.**	***T***	**P-Value**	**Coef.**	***T***	**P-Value**	**Coef.**	***T***	**P-Value**	**Coef.**	***T***	**P-Value**
Constant	35.53	1.162	0.275	7.94	0.421	0.684	-44.1	-4.38	0.001	608.628	2.586	0.024	17.0183	1.388	0.199
X_1	5.39	3.112	0.012	-6.0701	-5.67	0	-2.325	-4.07	0.002	12.34	0.881	0.396	-7.31	-10.519	0
X_2	-16.394	-1.38	0.29	-18.605	-2.54	0.032	3.786	5.38	0	-40.218	-2.49	0.028	40.41	8.485	0
X_3	-0.12903	-1.71	0.121	0.0291	0.625	0.547	0.1163	4.72	0.001	-1.075	-1.861	0.087	-0.04983	-1.65	0.133
$X_1 \times X_1$	0.127704	2.311	0.046	0.225	6.594	0	-0.0885	-4.87	-	-	-	-	0.0549	2.478	0.035
$X_2 \times X_2$	3.78967	2.44	0.037	7.1242	7.43	0	-	-	0	-	-	-	0.488487	0.784	0.453
$X_3 \times X_3$	0.001185	2.447	0.035	-3.2E-05	-1.08	0.307	-8E-05	-5.24	0.001	0.001	1.422	0.18	3.52E-05	1.835	0.1
$X_1 \times X_2$	-2.34484	-4.33	0.002	0.2171	0.649	0.532	-0.8433	-4.46	0	15.186	3.482	0.005	-2.04371	-9.406	0
$X_1 \times X_3$	-0.0063	-3.07	0.013	0.0048	3.77	0.004	0.00429	6.323	-	-0.025	-1.48	0.163	0.0103158	12.542	0
$X_2 \times X_3$	0.017489	1.239	0.247	0.0071	0.814	0.436	-	-	-	-	-	-	-0.04454	-7.866	0
R-Squared	99.20%			96.76%			94.45%			98.63%			98.62%		
P-Value of Lack-of-Fit	0.355			0.068			0.161			0.103			0.07		

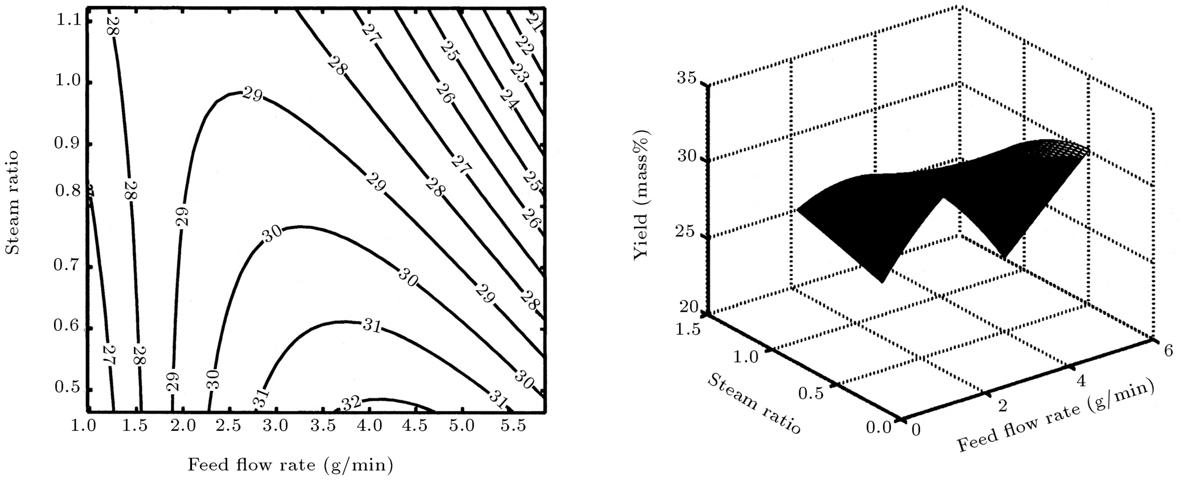

Figure 2. Dependence of ethylene yield on feed flow rate and steam ratio in uncoded levels. Response levels of ethylene yield are shown as contour lines.

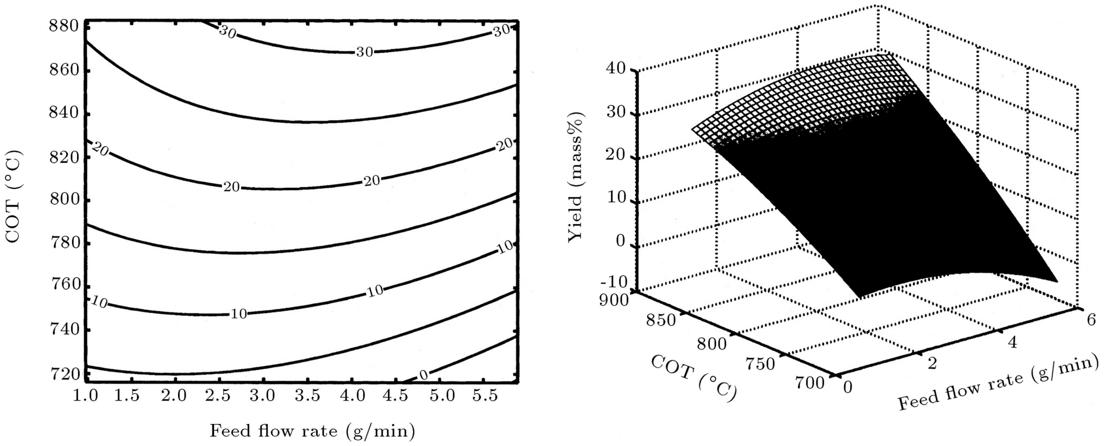

Figure 3. Dependence of ethylene yield on feed flow rate and COT in uncoded levels. Response levels of ethylene yield are shown as contour lines.

Figure 3 demonstrates the contour and surface of ethylene yield vs. variation of COT and feed flow rate at steam ratio of 0.46.

Contour lines of the demonstrated surface confirm that, at a constant feed flow rate and steam ratio, an increase in temperature results in an increase in ethylene yield. However, after a minimum point is reached, contour lines show an upward trend.

Figure 4 represents the surface and contour of ethylene yield vs. COT and steam ratio. It is revealed that, at a constant steam ratio, an increase in COT leads ethylene yield to be increased. The main reason for this is that the higher temperature increases the cracking rate.

Propylene plays a significant role in the net profit issue. Figures 5 to 7 demonstrate the trend of propylene yield vs. steam ratio, COT and feed flow rate.

In Figure 5 the surface and contours are divided into two main regions. In the first region, an increase in steam ratio increases the propylene yield at a constant feed flow. However, in the second region and at a constant feed flow rate, an increase in steam ratio decreases the yield of propylene.

Figures 6 and 7 illustrate the dependency of the propylene yield on the feed flow rate, COT and steam ratio. As can be seen, increasing COT at a constant feed flow rate increases the yield of propylene. After reaching the maximum level, it would have a decreasing trend.

Figures 8 and 9 indicate the trend of surface and contour lines of butadiene yield vs. COT, feed flow rate and steam ratio.

These figures show that an increase in COT at a constant feed flow rate and steam ratio increases the yield of butadiene. However, at constant steam ratio and COT, an increase in feed flow rate would decrease the yield of butadiene.

The trends of butene yield are shown in Figures 10 and 11. Figure 10 shows the contour lines of the

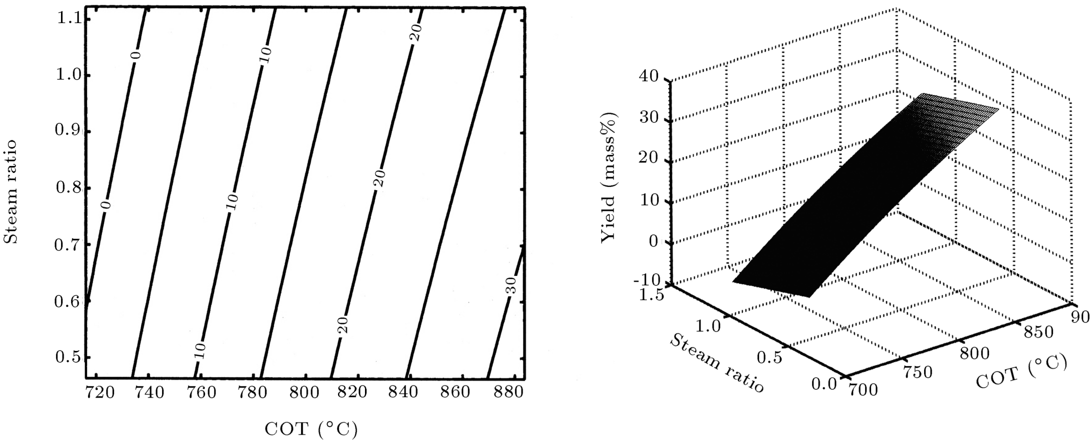

Figure 4. Dependence of ethylene yield on COT and steam ratio in uncoded levels. Response levels of ethylene yield are shown as contour lines.

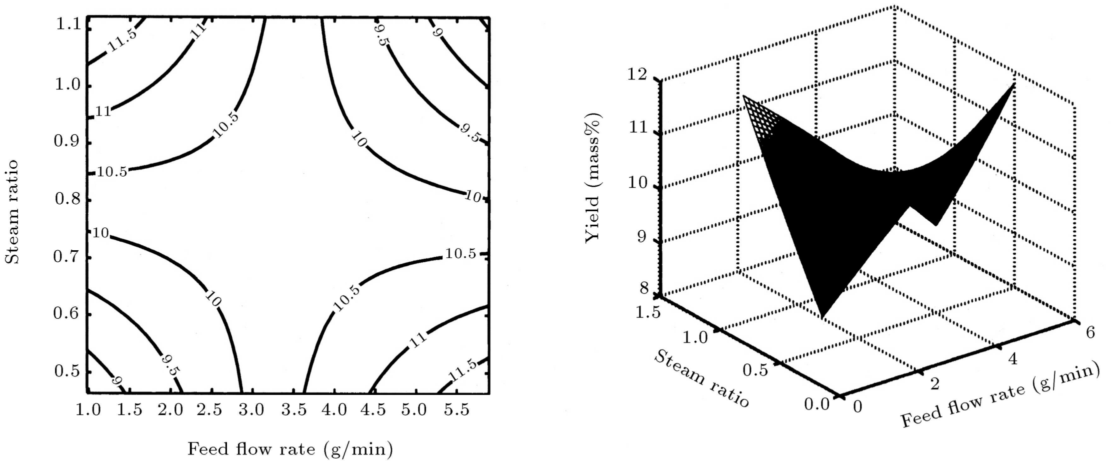

Figure 5. Dependence of propylene yield on feed flow rate and steam ratio in uncoded levels. Response levels of the propylene yield are shown as contour lines.

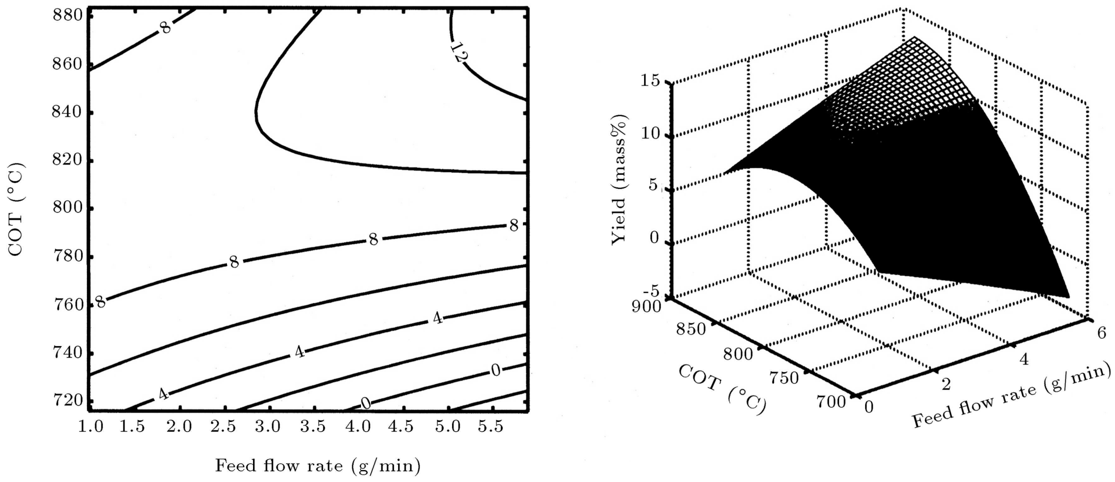

Figure 6. Dependence of propylene yield on feed flow rate and COT in uncoded levels. Response levels of propylene yield are shown as contour lines.

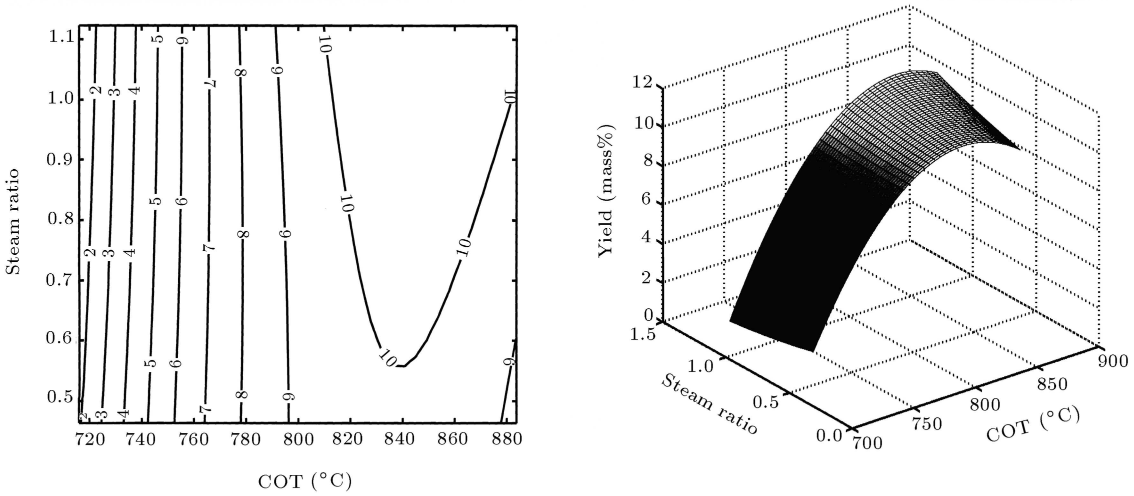

Figure 7. Dependence of propylene yield on COT and steam ratio in uncoded levels. Response levels of propylene yield are shown as contour lines.

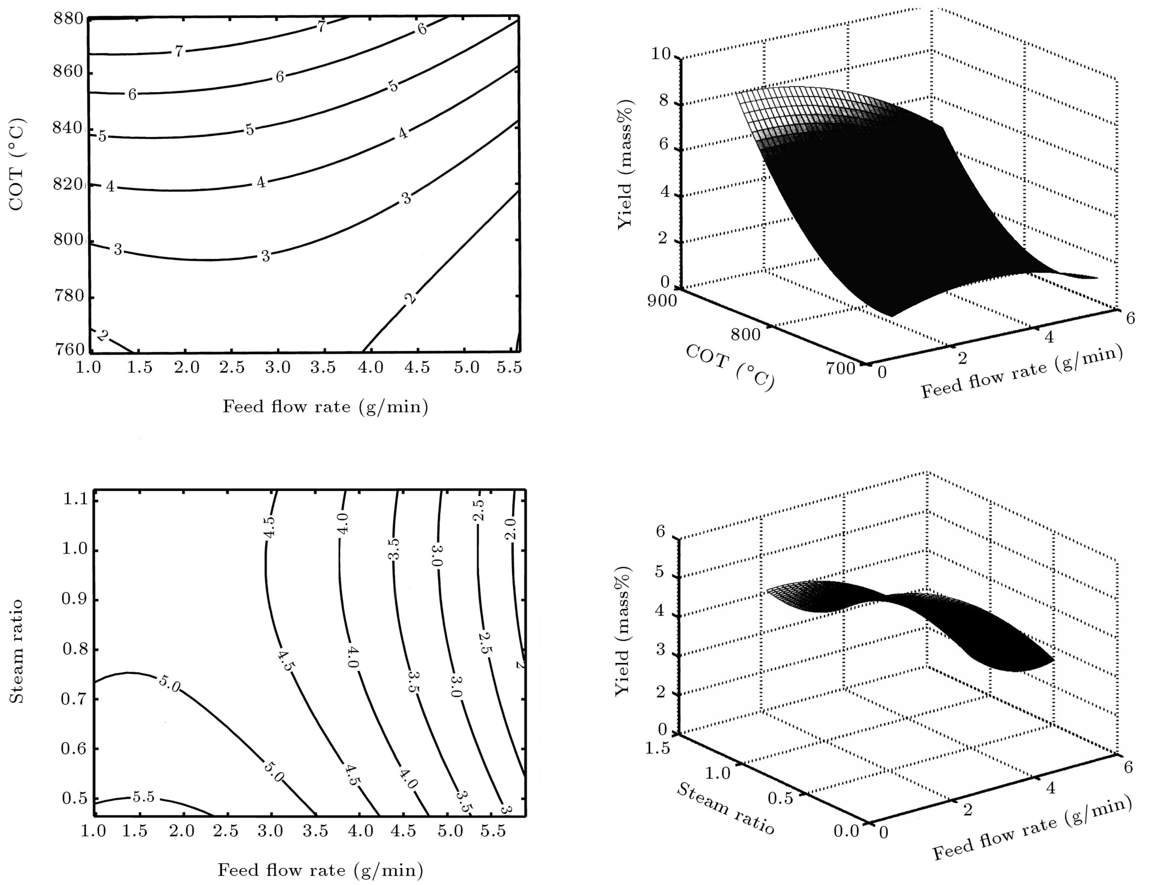

Figure 8. Dependence of butadiene yield on feed flow rate, COT and the steam ratio in uncoded levels. Response levels of butadiene yield are shown as contour lines.

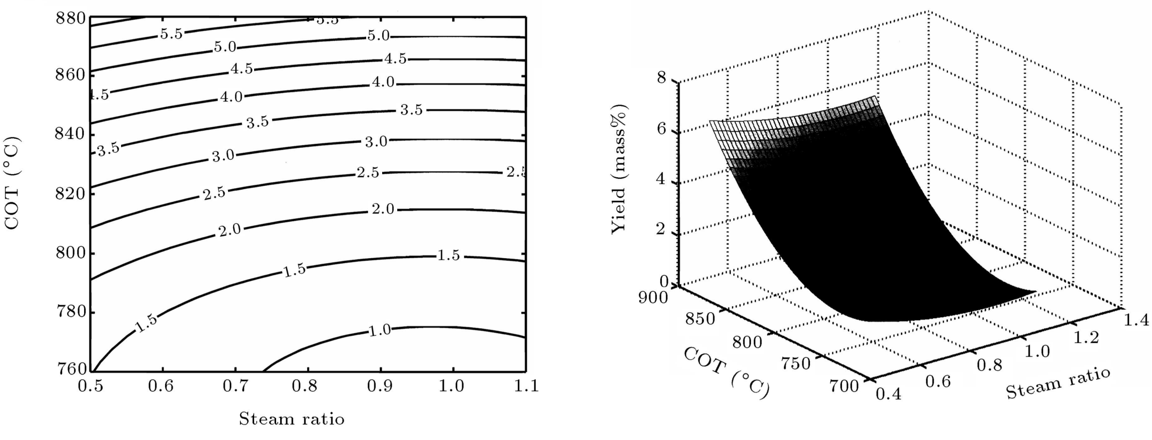

Figure 9. Dependence of the butadiene yield on the COT and steam ratio in uncoded levels. Response levels of the butadiene yield are shown as contour lines.

butene yield when the COT and feed flow rate are varied. Figure 11 demonstrates the dependency of the production yield of butene on the steam ratio and feed flow rate. It is shown that, at constant temperature, an increase in feed flow rate would consequently decrease the butene yield. Nevertheless an increase in COT at constant feed flow rate would increase the butene at a constant steam ratio. It was also revealed that, at constant steam ratio, an increase in feed flow rate will decrease the butene yield.

The rate of coke formation is the last studied response variable. The coke formation is always accompanied by a great economic loss. So, a decrease in coke formation is always a field of interest in the

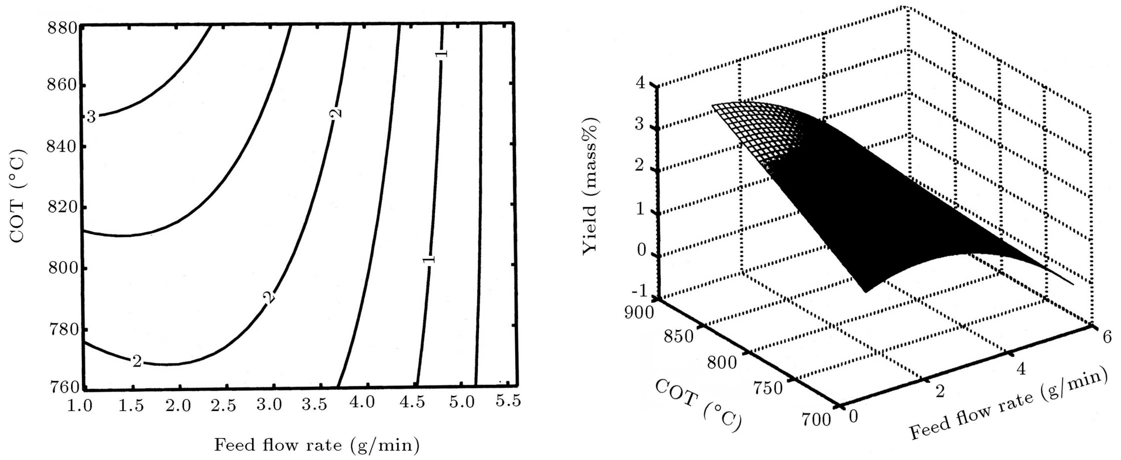

Figure 10. Dependence of butene yield on the COT and feed flow rate in uncoded levels. Response levels of the butene yield are shown as contour lines.

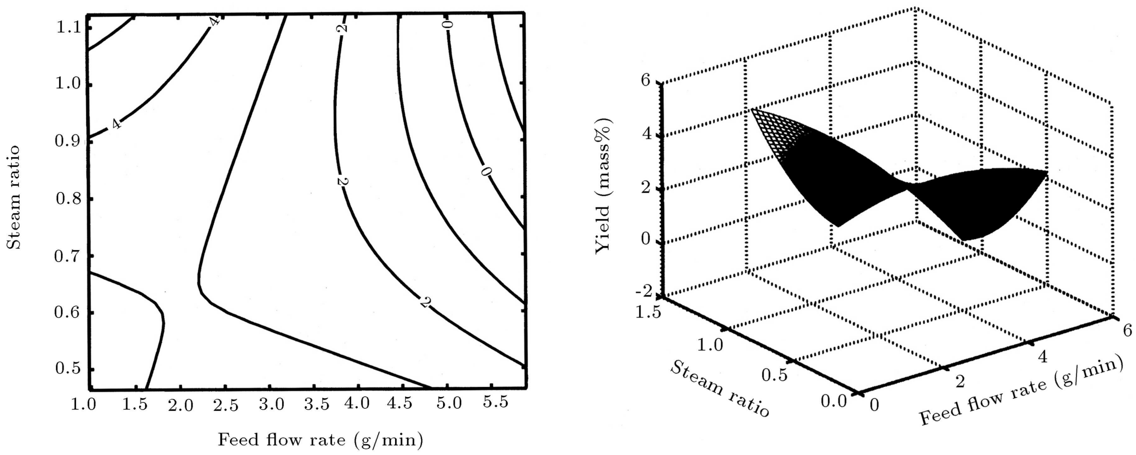

Figure 11. Dependence of butene yield on the steam ratio and feed flow rate in uncoded levels at COT of 885°C. Response levels of the butene yield are shown as contour lines.

thermal cracking of hydrocarbons.

First, the trends of the rate of coke formation should be determined. Figures 12, 13 and 14 show the dependency of the rate of coke formation on the COT, feed flow rate and steam ratio. These figures reveal that a rising in COT, increases the rate of coke formation. However, an increase in the steam ratio and feed flow rate would decrease the rate of coke formation.

Every trend of the contour lines can be interpreted with regard to the nature of pyrolysis reactions of hydrocarbons. The pyrolysis reactions are divided into two main groups: As primary and secondary reactions. The primary reactions are defined as the reactions which primarily occur in the pyrolysis of hydrocarbons and the secondary reactions are defined as the subsequent reactions of products formed in the primary reactions [14]. The primary reactions mainly occur in the first stages of pyrolysis. As the residence time is prolonged and the temperature rises , the conversion of the hydrocarbons feed stock is increased and the products of the primary reactions gradually grow. Subsequently, the secondary reactions are conducted when the primary reactions of the unconverted feedstock are still occurring. A quantitative increase in primary products would raise the secondary reaction rates. This would result in a decrease in the primary products and an increase in the secondary products.

The effects of feed flow rate and steam ratio on the yields of primary products are illustrated in Figures 2 and 5. The trend of contour lines and surfaces in these two figures confirm the effects of the feed flow rate and the steam ratio on the yield of ethylene and propylene as primary products. At a constant steam ratio, an increase in feed flow rate would decrease the residence time. At first, it decreases the reaction rate of formation of the secondary products, then in the range of higher feed flow rates, it reduces the primary products. An increase in the steam ratio, at a constant feed flow rate, decreases the residence time and partial pressure of the reactants. Consequently,

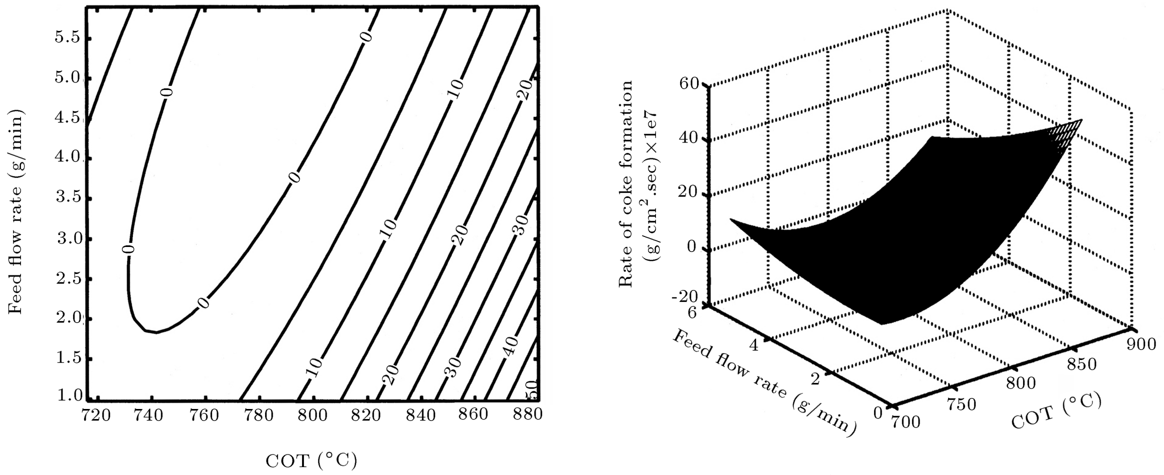

Figure 12. Dependence of the rate of coke formation on the feed flow rate and COT in uncoded levels at steam ratio of 0.80. Response levels of the yield of coke are shown as contour lines.

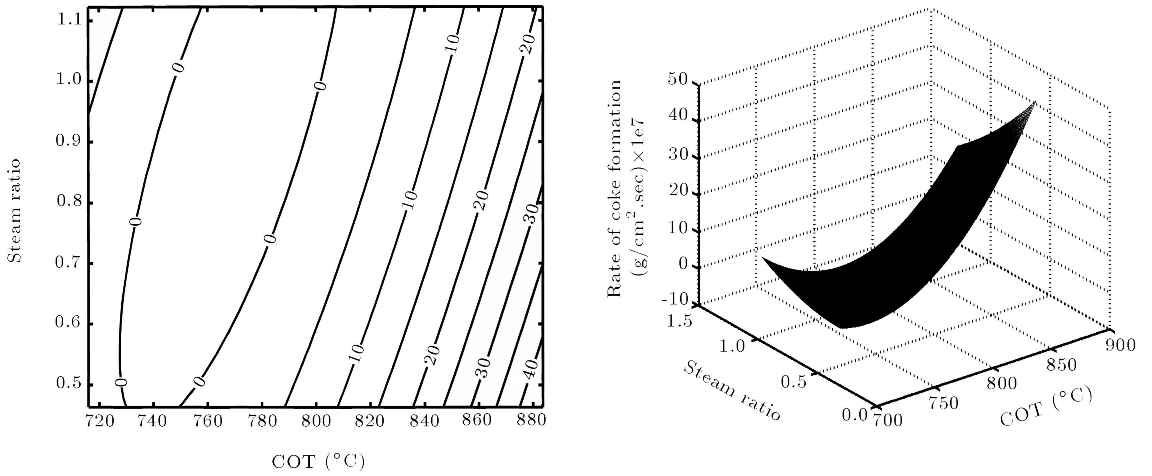

Figure 13. Dependence of the rate of coke formation on the steam ratio and COT in uncoded levels at a feed flow rate of 3.5 gr/min. Response levels of the rate of coke formation are shown as contour lines.

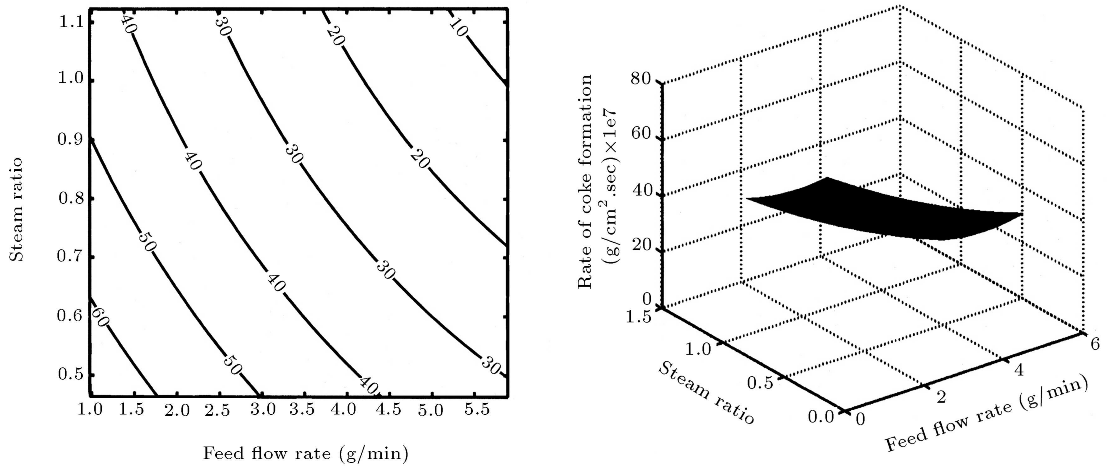

Figure 14. The response surface plot of the rate of coke formation as a function of feed flow rate and steam ratio at COT of 885°C.

it decreases the yield of the secondary products and increases the yield of primary products when the residence time is high. It also affects all the reaction rates and decreases the yield production of primary and secondary products when the residence time is low.

Determination of the optimum condition is one of the main challenges in chemical processes. Defining a suitable objective function is the first step in optimization. This research concerns the maximization of the net profit of the process as a target. Accordingly, the objective function is defined as follows:

$$\text{f} = \text{income} - \text{cost}. \tag{2}$$

Income is the sale price of the desired products. The desired products are ethylene, propylene, butadiene, butenes and light gases which are paraffinic light gases and hydrogen. The price of each of these groups [15,16] is listed in Table 5. The costs of the production include cost of decoking and energy consumption during the thermal cracking.

By applying the data from Table 5 and the aforementioned statistical models in the form of Equation 1, Equation 2 can be consequently extended. Accordingly, the income part of the objective function is shown as follows:

$$\begin{aligned}\text{Income} = {} & 6 \times 10^{-4} \times X_1 \times (1.15 \times Y_{\text{Ethylene}} + 1.16 \\ & \times Y_{\text{Propylene}} + 0.831 \times Y_{\text{butadiene}} + 0.35243 \\ & \times Y_{\text{butenes}} + 0.266 \times Y_{\text{fueloil}} + 0.5747 \times Y_{\text{LG}} \\ & + 0.95 \times Y_{\text{Acetylene}}).\end{aligned} \tag{3}$$

Regarding radiation as the main mechanism of the heat transfer and the power consumption of the compressor in the decoking period, the cost part of the objective function is as follows:

$$\begin{aligned}\text{Cost} = {} & 2.64 \times 10^{-4} \times X_1 \times X_2 + 9.041 \times 10^{-14} \\ & \times ((X_3 + 1266)^4 - (X_3 + 1066)^4) \times (1 + \lambda) \\ & + 0.0671 \times \lambda.\end{aligned} \tag{4}$$

λ is an empirical factor predicting the relationship between the required time for decoking and the operating time. It is defined as the ratio of the decoking period (numerator) over the main process period (denominator). In fact, the decoking period increases the cost of production by the utilization of air and energy to burn the coke.

In order to consider the cost of the decoking period time in net profit calculations, the empirical factor is defined. The value of this parameter is varied and depends on the consumed air, the temperature profile of the reactor along the decoking period and the amount of coke formed during the thermal cracking process. With regard to the conducted experiments, the value of this parameter is varied and is between 0.1 to 0.75(hr/hr) for the thermal cracking of atmospheric gasoil in the developed pilot plant.

The optimization is accompanied by some constraints. At first, the reactor temperature must be set less than 890°C, due to some metallurgical concerns. The range of the flow rate of the feed and water should also be between 1 and 6.5 (gr/min). In addition, the yield of each product must be between 0% to 100% and, in regard to the principle of mass conservation, the total mass of effluent of the reactor must be equal to the total mass entering the reactor.

In order to solve the problem, the SQP method has been applied. Table 6 shows the optimum conditions and the yield of the main products.

Table 5. Product values and operating costs [15,16].

Item	Value
Power (\$/kWh)	0.06
Feed (\$/kg)	0.525762
Acetylene (\$/kg)	0.95
Ethylene (\$/kg)	1.150
Propylene (\$/kg)	1.160
Butadiene (\$/kg)	0.831
Butenes (\$/kg)	0.35243
Deionized water (\$/kg)	0.0044
Fuel oil (\$/kg)	0.266
Light gases (\$/kg)	0.5747

Table 6. The optimum operating conditions and yield of products for the developed pilot plant.

Operating Condition	Value
Temperature (°C)	843.8
Feed flow rate (gr/min)	6.02
Steam ratio	0.46
Residence time (sec)	0.3
$Y_{\text{Acetylene}}$ (%)	1.0626
Y_{Ethylene} (%)	23.82
$Y_{\text{Propylene}}$ (%)	12.13
$Y_{\text{Butadiene}}$ (%)	2.42
Y_{Butenes} (%)	2.45
Y_{LG} (%)	6.122
$Y_{\text{fuel oil}}$ (%)	51.9
Rate of coke formation (gr/cm^2.sec)$\times 10^7$	14.44

CONCLUSION

Based on the central composite design method, 19 experiments (15 experiments combined with four replications) were designed to study the effects of different operating parameters and their interactions on the yield of thermal cracking products of chosen atmospheric gasoil. Statistical models for the prediction of the yield of selected products of the thermal cracking of this feedstock were developed and evaluated. The contours and surfaces of the yields of the selected products had different trends, depending upon the operating conditions. In most cases, increasing the temperature enhances the yield of the products. In some cases, by increasing the temperature, the yield of the products reaches the maximum point and afterwards has a decreasing trend. A rising feed flow rate and steam ratio usually decreases the yield of the products.

Based on the developed models, a constrained optimization was carried out to maximize the net profit of the operation. At the optimum point, the yield of ethylene, propylene and butadiene were, respectively, 23.82%, 12.13% and 2.42%.

ACKNOWLEDGMENTS

The financial support provided by the Research and Development Center of the National Petrochemical Company is greatly appreciated.

NOMENCLATURE

COT	coil outlet temperature (°C)
Coef.	coefficient in quadratic model
T_{furnace}	temperature of reactor furnace (K)
T_{skin}	skin temperature of the reactor (K)
XOT	cross over temperature (°C)
X_1	experimental design parameter (feed flow rate (gr/min))
X_2	experimental design parameter (steam ratio)
X_3	coil outlet temperature (°C)
Y_i	yield of products (mass %)
α	constant coefficient in quadratic model
β_{ij}	coefficients in quadratic model
λ	experimental factor for predicting the relationship between decoking time and operating time (hr/hr)

REFERENCES

1. Niaei, A., Towfighi, J., Sadreameli, S.M. and Karimzadeh, R. "The combined simulation of heat transfer and pyrolysis reactions in industrial cracking furnaces", *Applied Thermal Engineering*, **24**, pp 2251-2265 (2004).
2. Sadreameli, S.M. and Green, A.E.S. "Systematic and modeling representation of naphtha thermal cracking for olefin production", *Journal of Analytical and Applied Pyrolysis*, **73**, pp 305-313 (2005).
3. Masoumi, M.E., Sadreameli, S.M., Towfighi, J. and Niaei, A. "Simulation, optimization and control of a thermal cracking furnace", *Energy*, **31**, pp 516-527 (2006).
4. Grace Chan, K.Y., Inal, F. and Senkan, S. "Suppression of coke formation in the steam cracking of Alkanes", *I & EC Research*, **37**, pp 1125-1132 (1998).
5. Manafzadeh, H., Sadreameli, S.M. and Towfighi, J. "Coke deposition by physical condensation of polycyclic hydrocarbons in the transfer line exchanger (TLX) of the olefin plant", *Applied Thermal Engineering*, **23**, pp 1347-1358 (2003).
6. Zdonik, S.B., Hayward, G.L. and Fishtine, S.H. "Olefins production by gas oil cracking", *Hydrocarbon Processing*, pp 32-35 (Dec. 1975).
7. Kaiser, V., Gilbourne, D. and Pocini, C.A. "Analyze steam cracker economics", *Hydrocarbon Processing* (April 1977).
8. Depeyre, D., Flicoteaus, C., Arabzadeh, F. and Zabaniotou, A. "Modeling of thermal steam cracking of an atmospheric gas oil", *I & Eng. Chem. Res.*, **28**(7), pp 1476-1483 (1989).
9. Clymans, P.J., Froment, G.F., Berthelin, M. and Trambouze, P. "Olefins and BTX-production by thermal cracking of hydrotreated vaccum gas oil and related fractions", *AIChE Journal*, **30**(6) pp 904-914 (1983).
10. Wernike, et al. "Thermal cracking of heavy fraction of hydrocarbon hydrogenate", *U.S. Patent* (4260474) (April 7, 1981).
11. Albright, L.F., Crynes, B.L. and Corcoran, W.H., *Pyrolysis: Theory and Industrial Practice*, Academic Press (1983).
12. Davies, L., *Efficiency in Research Development, and Production: The Statistical Design and Analysis of Chemical Experiments*, The Royal Society of Chemistry (1993).
13. Seber, G.A.F. and Wild, C.J., *Nonlinear Regression*, John Wiley & Sons, Inc 2003).
14. Zou, R., *Fundamentals of Pyrolysis in Petrochemistry and Technology*, Lewis Pub. (1993)
15. "The price of different products", http://WWW.nioc.org/publications/fanavari/findex.asp
16. Mohaddecy, R.S., Sadighi, S., Zahedi, S. and Bahmani, M. "LP modeling of Tehran refinery to maximize the net profit", *Technical Report*, Tehran Refinery (2006).